Optimization of Tilt, List, and Skew of Sea-to-Shore Gantry Cranes

Martin N. Mae[1,3*], Michael J. Saulo[1], Michael D. Odhiambo[1], Daniel N. Wang'ombe[2]

[1]Department of Electrical and Electronic Engineering, Technical University of Mombasa, P.O Box 90420-80100 Mombasa, Kenya; [2]Department of Mechanical and Automotive Engineering, Technical University of Mombasa, P.O Box 90420-80100 Mombasa, Kenya; [3]Kenya Ports Authority P.O Box 95009-80400 Mombasa, Kenya

*Corresponding author's email: martinngumbao@yahoo.com

Abstract

Automation of sea-to-shore gantry cranes and use of artificial intelligence is a trend that most ports are trying to adopt in order to cope with handling of high volume of containerized cargo. Low target achievements in container handling have resulted in low ship turn around. The aim of automation was to either offload or load high volumes of containers in order to increase productivity and ship turn around. This study developed a vision-based real-time monitoring system integrated with an adaptive PID controller to detect tilt, list, and skew of spreader in sea to shore gantry cranes with high accuracy. The system integrated cameras, counters, sensors, and encoders that enable real-time monitoring and control of movements of cranes. A mathematical model was developed to describe a three-dimensional movement of a crane spreader in order to perfect tilt, list and skew. Due to automation, the time to handle a container reduced from 8 min to 2.5 min. This resulted into crane performance improvement of 68.8%. The developed monitoring system reduced operational time, enhanced safety and reduced costs.

Key Words: Corner cast, Spreader, Port, Quay, Gantry crane, PID

Introduction

Containerized cargos play a central role in transportation of goods, with a significant volume of containers being handled at container ports. Sea-to-shore cranes are frequently utilized to transport containerized cargo from quay side to a ship and vice versa (Jaafar et al., 2013). With the increasing volume of containers being processed, there has been a rising demand for these cranes to operate at larger capacities and faster speeds to meet the targets (Ngo et al., n.d.; Grypp et al., 2014). The spreader in sea-shore gantry crane presents a critical component, serving as the interface between lifting equipment and ISO standard containers (Masoud et al., 2004). The precise control of spreader tilt has emerged as a fundamental requirement for safe and efficient sea to shore operations particularly as container ships increase in size and port throughput demands escalate (Milazzo et al., n.d.). Tilt angle control addresses multiple operational challenges in container placement (Armstrong et al., n.d.). During loading and offloading of containers, spreader must maintain its level of orientation despite external variables like wave induced motion, wind, and crane dynamics (Kim & Hong, 2019). For bulky materials handling application, active tilting enables efficient unloading of granular cargo through controlled container tipping (Ayper & Pense, 2026).

The global intermodal stands as the backbone of modern supply chain, facilitating the transport of over 1.8 billion metric tons of goods annually (Kugler et al., 2021). The efficiency of this intricate network hinges on the seamless transfer of container from the ship, trucks, trains and storage yards, a process dominated by gantry cranes (Bruggeling, n.d.). At the heart of this operation lies the spreader the specialized lifting attachment that forms the critical interface between twist locks and the container (Qian et al., 2018). The precise and efficient placement is not merely a function of crane operator skill. This was fundamentally governed by a dynamic behavior of the spreader particularly its ability to control the listing angle (Ngo et al., n.d.). List angle is the deviation of spreader from a horizontal plane typically about its longitudinal axis (Li et al., 2022). It has direct impact on

Published, June 2026

operational safety, structural integrity and throughput (Milazzo et al., n.d.). An uncontrolled or excessive listing during landing can lead to misalignment with corner castings resulting in costly delays, accelerated wear on guide system and in worse-case scenario, catastrophic container drops or damage to both the cargo and the vessel or terminal infrastructure (Yılmaz, 2023).

On the other hand, the effectiveness of skew depends critically on the transformation between actuator displacement and resulting spreader rotation angle (Smid et al., 2000; Ngo & Hong, 2009). This transformation expressed mathematically as kinetic conversion factor varies with hoist heights, spreader configuration (20ft, 40ft, 45ft) and the geometric characteristic of the suspension system(Cibicik et al., 2018; Galeani et al., 2008). The objective here was to achieve perfect spreader twist locks landing in to container corner casts within the shortest time possible. To achieve it, the tilt list and skew angle transformation parameters were supposed to be symmetrically optimized to minimize residual and maximize sea-to-shore (STS) crane productivity by reducing the time cycle per move and the approached method used to solve it.

Historically, container handling relied heavily on operator expertise to visually correct for tilt, list, and skew induced by asymmetric loads, wind gusts or inertia forces darling crane movements. However, the modern era of automated and semi-automated terminals, characterized by proliferation of automated staking cranes (ASCs) and Ship-to-shore (STS) cranes demand a new paradigm shift (Beller & Yavuz, 2021; Parra & Tannuri, 2012). Some cranes in the developing world have not yet adopted the fully autonomous of their gantry crane as technology keeps on advancing, making them record low performance in productivity. Moreover, automation is a performance choice by empowering people with better tools and better data. The push for remote and full automation has placed stringent requirements on the precision of the spreader's final positioning, where tolerances are often measured in degrees and within the shortest time possible. Consequently, the active control of the tilt, list, and skew angle has emerged from niche area of mechanical design to a central focus in control system, sensor fusion and operational research within port automation (Zhou et al., n.d.). This paper provides a comprehensive experimental outcome of the tilt, list and skew angle in container placement using spreader in 3 seconds and 3 min per move from 9 min.

Methodology

Proposed System design

The spreader had the ability to track position of the container corner castings in 3 sec. A total of 6 AI cameras were set under the spreader, as the crane spreader descended from an initial height of 30 m to a target container height of 2 m at a maximum descent speed of 1.6 m/s. During descent, at approximately 7 m, a machine vision systemd (camera + image processing algorithm) was activated. The cameras captured 3D images of the spreader in real time, reconstructing its position to detect any tilt, list or skew, deviation (Figure 1). The captured images were sent to a central processing computer which analyzed them and determined the extent of deviation. Upon detecting a tilt, list, or skew deviation, a control command was issued to adjust the spreader's orientation.

Published, June 2026

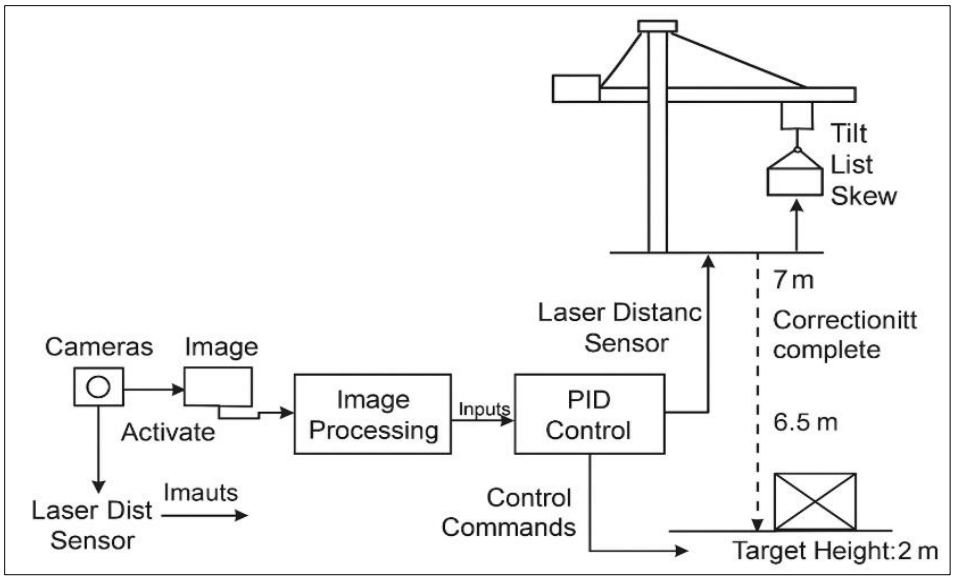

Figure 1. Designed communication pathway between spreader and the cameras used during the experimental study

In the MATLAB Simulink model, the Machine Vision operation was represented by an idealized detection process, whereby a step input deviation of 3° was introduced at exactly 6.5 m height and this deviation was fed into the PID controller for correction. The PID controller processed the deviation and commanded the hydraulic actuator system (modeled through dynamic response blocks) to correct the spreader's orientation before it reached the container. The spreader had 4 pulleys attached to it which were rotated by wire ropes during lifting and lowering of the spreader. Here, the spreader was simply suspended by the wire ropes. The wire ropes were fixed to a rotating drum from the machine house and passed through the back-reach pulleys, then to the spreader pulleys to a boom top. The back-reach pulleys were held by hydraulic cylinders which could be shifted from time to time and by doing so tilt, list and skew of the spreader was achieved based on the position of the container. To achieve this, the cameras were activated by the laser sensor which captured the corner casts position of the container and transferred them as images to the central processing unit (CPU) (Figure 2). This system detected a reference point on how to align the spreader twist locks to couple the container. This was achieved by shifting the hydraulic actuators based on the input reference point as registered by the proportional integral gain. The spreader had twist locks which coupled the container. The operator's seat was equipped with push buttons used to adjust the spreader twist locks to align with the container corner casts. By using the push buttons the shifting of the hydraulic cylinders was done hence achieving the tilt, list and skew motions.

Published, June 2026

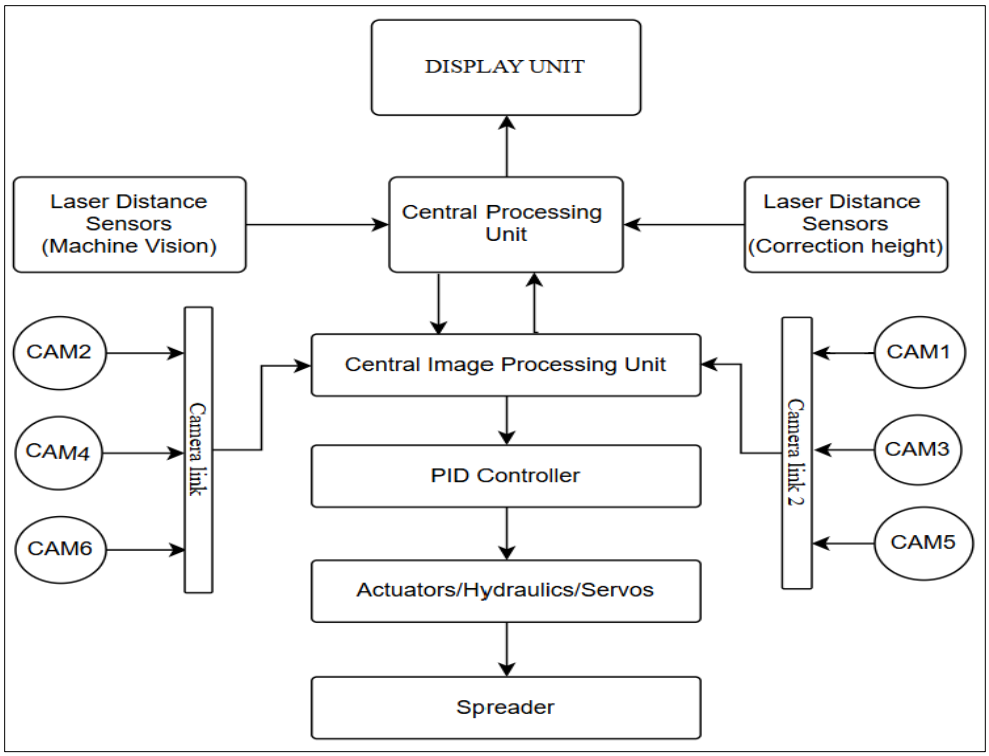

Figure 2. Image processing from camera to the CPU and spreader

The natural dynamic behavior of the spreader-crane system was captured using a second-order transfer function. This accounted for realistic effects such as inertia, oscillations, and response delays. Practical effects like machine vision processing time and hydraulic actuator delays (modeled as ~0.1s delay) were included to simulate real-world latency in correction signals. When during operation, the spreader tilt, list and skew angle exceeded acceptable thresholds, a fault detection logic was triggered. This enabled emergency responses or alarms and prevented unsafe container handling. Between 7 and 6.5 m of descent, the machine vision system remained active, confirming spreader alignment and detected any deviations. Below 6.5 m, the system finalized corrections using the last valid machine vision reading, allowing complete correction within the available settling time (~2.8 s).

Establishment of Tilt, List and Skew Models

The tilt, list and skew were then amalgamated by an integrator logic control unit for a desired smooth output (Figure 3).

Published, June 2026

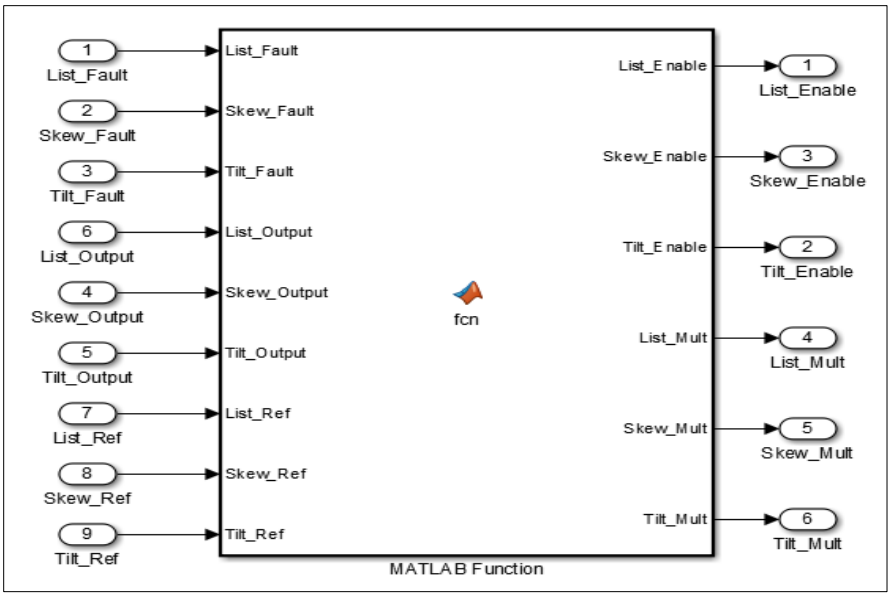

Figure 3. Tilt, list, and skew integrator unit

Each motion had its own reference point. For tilt, the reference point was -2 degrees, for list and skew was 2 degrees each. For the tilt angle to function (Figure 4), the reference point of -2 degrees was in scope 1, as demonstrated in the MATLAB result purposely for tilt standalone.

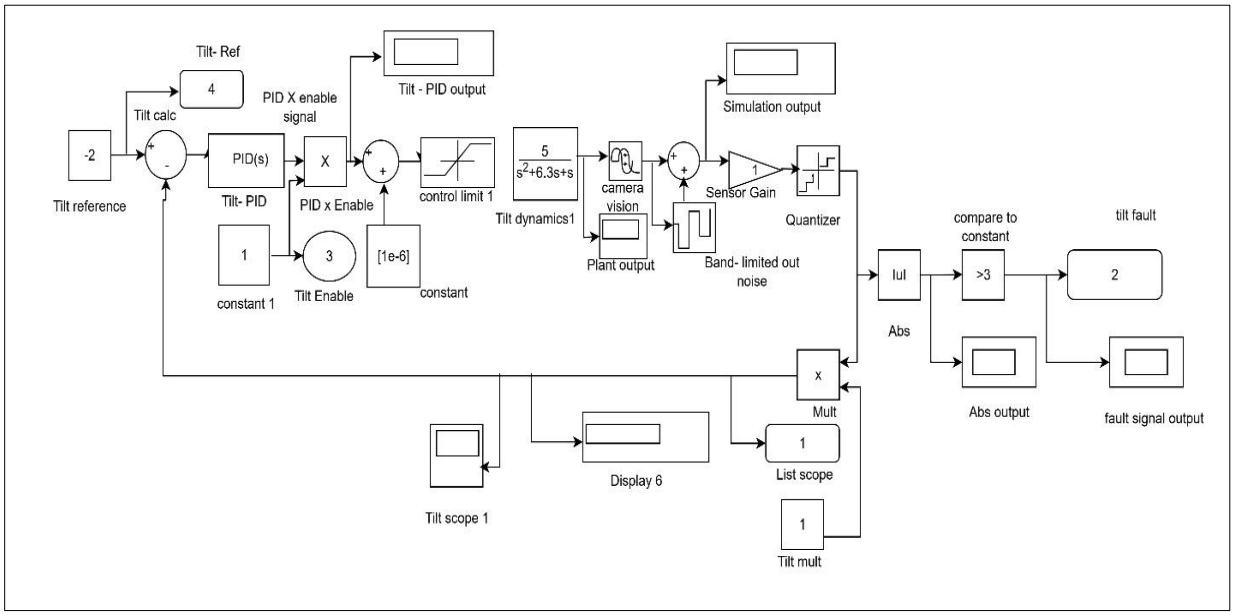

Figure 4. Stand-alone tilt control system

The tilt stand-alone, list stand-alone, and skew stand-alone were fused in the integrator unit. This unit had 3 reference points, a plant and a correction unit. This means the correction unit made the spreader at 0 degrees before camera was activated (Figures 4, 5 and 6), and these were amalgamated by the integrator system for smooth output.

System Parameters

The PID Controller Parameters, continuously calculated the error value between the desired

Published, June 2026

targeted set point, and the measured process variable and a correction was applied to keep the system stable and accurate.

From Figure 4 parameters, the system had a Proportional Gain K_p of 1.6, Integral Gain K_i of 1.9, Derivative Gain K_d = 0.09

Plant Transfer Function

The plant transfer function $\boldsymbol{G_P(s)}$ was given by the following equation**:**

$$G_P(s) = \frac{5}{s^2+6.3s+5} \quad (1)$$

Equation 1 presented the plant which had an effect on spreader alignment based on reference point.

Transport Delay

The transport delay introduced by the Machine Vision system was denoted by T_d, typically in the range of 100–200 ms. Given that:

T_d = 0.15 seconds

This delay was modeled as an exponential in the Laplace domain using the following equation:

$$G_d(s) = e^{-Td^S} \quad (2)$$

PID Controller Transfer Function

The standard form of a PID controller in the Laplace domain was given by:

$$G_C(s) = K_P + \frac{K_I}{S} + K_D s \quad (3)$$

Substituting values:

$$G_C(s) = 1.6 + \frac{1.9}{S} + 0.09s \quad (4)$$

$$= \frac{0.09S^2+1{\cdot}6S+1{\cdot}9}{S} \quad (5)$$

Open-Loop Transfer Function

The open-loop transfer function $G_{OL}(s)$ of the system including controller, plant, and delay was given by:

$$G_{OL}(s) = G_C(s).\ G_P(s).\ G_d(s) \quad (6)$$

Substituting the values

$$G_{OL}(s) = \frac{0.09S^2+1{\cdot}6S+1{\cdot}9}{S} \cdot \frac{5}{s^2+6.3s+5} \cdot e^{-0.15s} \quad (7)$$

Closed-Loop Transfer Function

Let $G(s) = G_C(s).\ G_P(s).\ G_d(s)$, then the closed-loop system transfer function was expressed following,

$$T_{(s)} = \frac{G_{(s)}}{1+G_{(s)}} = \frac{G_{OL}(s)}{1+G_{OL}(s)} \quad (8)$$

However, due to the presence of a transport delay, the system became a non-rational transfer function (non-polynomial due to e^{-sT}. This implied:

Classical Laplace-domain analysis tools (like root locus or frequency response) were approximate. Time-domain simulations or Pade approximation is used for practical analysis.

Pade Approximation for Transport Delay

To facilitate simulation and analysis, we approximated to e^{-Td^S} using a first-order Pade approximation following the equation:

$$e^{-Td^s} \approx \frac{1-\frac{T_d}{2}s}{1+\frac{T_d}{2}s} \quad (9)$$

Substituting T_d = 0.15 seconds

$$e^{-0.15\,s} \approx \frac{1-0.075s}{1+0.75s} \quad (10)$$

Now the full rationalized open-loop transfer function became:

$$G_{OL}(s) = \left(\frac{0.09s^2+1{\cdot}6s+1{\cdot}9}{s}\right) \cdot \left(\frac{5}{s^2+6{\cdot}3s+5}\right) \cdot \left(\frac{1-0.075s}{1+0.075s}\right) \quad (11)$$

Final Transfer Function Summary

$$G_{OL}(s) = 5\left(\frac{0.09s^2+1{\cdot}6s+1{\cdot}9(1-0.075s}{s(s^2+6{\cdot}3s+5)(1+0.075s)}\right) \quad (12)$$

This transfer function can now be used for stability analysis (e.g. Routh-Hurwitz or Nyquist).

In an open-loop dynamic system, the control dynamic system behaved as in the equation below before feedback correction was applied.

List Simulation in Simulink

With a reference point of 2 degrees the list command was activated when the spreader was at 0 degrees (Figure 5).

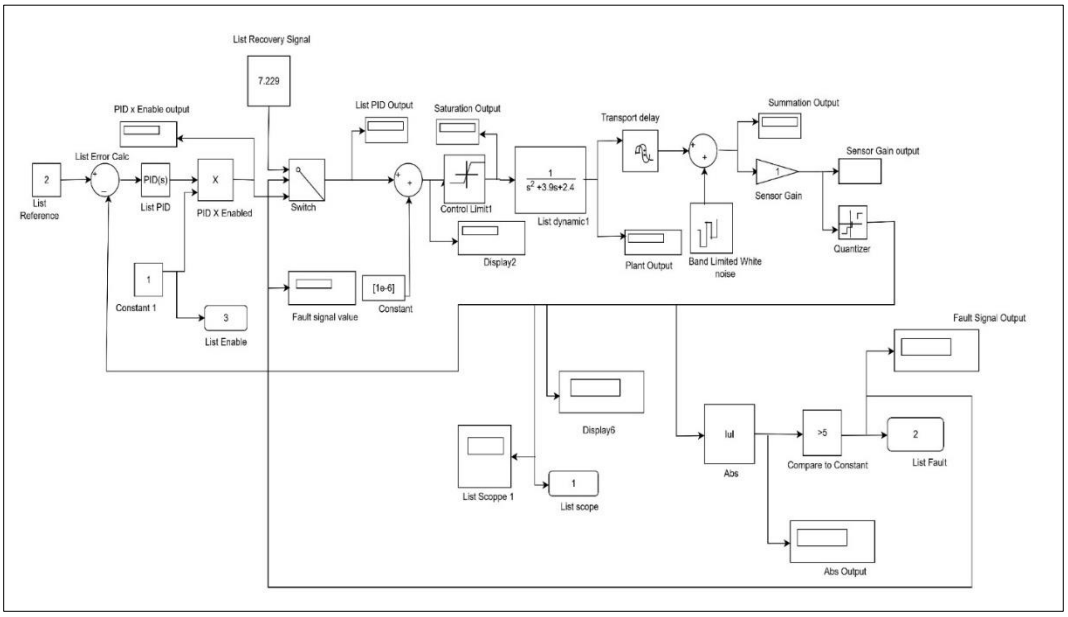

Figure 5. list standalone control system

The skew angle $\theta_s(t)$represented the misalignment, and we modeled the plant dynamics for skew correction as a second-order linear system derived from system identification or physical modeling. The plant and refence point affected the outcome (Figure 6).

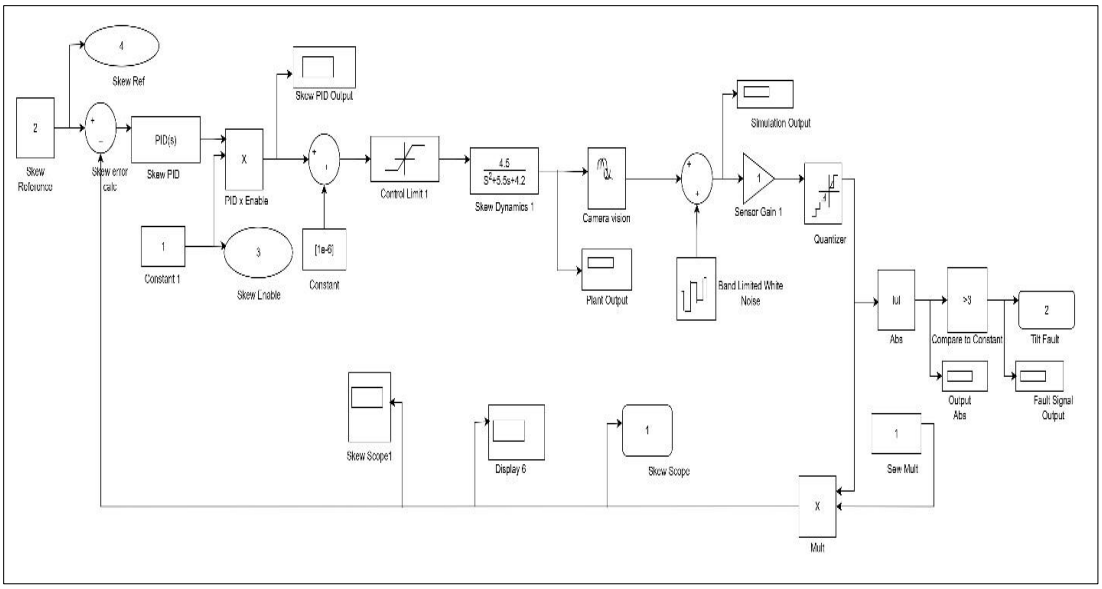

Figure 6. The skew stand-alone with skew scope1 for display

Controller Transfer Function

A PID controller was applied to minimize list deviation using the following equation:

$$C(s) = K_P + \frac{K_i}{s} + K_d s = 3 \cdot 2 + \frac{2 \cdot 6}{s} + 0.03s \tag{13}$$

Closed-Loop with Delay

To incorporate sensor and hydraulic actuation delays (0.1 s each), the total loop included a transport delay term represented by the following equation:

$$G_d(s) = \frac{C(s)P(s) \cdot e^{-Tds}}{1 + C(s)P(s) \cdot e^{-Tds}} \quad , \; T_d = 0 \cdot 1\text{s} \tag{14}$$

Simulation Methodology

The spreader was at 30m above the ground and the target was 2m as the height of a container at a speed of 1.6m/s (Figure 8).

The simulation was run using MATLAB Simulink command on the closed-loop system. A 3° list deviation was applied as a step input at a height of 6.5 m. The total descent time and available correction window were represented as follows:

Total descent time: $t_{total} = \frac{30-2}{1.6} \approx 17.5s$ (15)

Correction window: $t_{correction} = \frac{6.5-2}{1.6} \approx 2.8125\text{s}$ (16)

Correction Efficiency = $\left(\frac{\theta_{initial} - \theta_{final}}{\theta_{initial}}\right) \times 100$ (17)

Correction Efficiency: $E_{ffiency} = \frac{3-0.0013556}{3} . 100 \approx 99.9548\%$ (18)

Results and Discussion

Tilt, list, and skew angle simulation movement

The tilt, list and skew control stabilization subsystem was responsible for maintaining the tilt, list and skew stability of the ship-to-shore (STS) gantry crane spreader at 2 or 3 degree which was the reference point. Within 2.5 sec the system was at its peak and within 4.1 sec the system output was stable (Figure 7) which showed the reference angle against time taken to perfect the spreader auto-alignment. Figure 8 demonstrated the movement of the spreader targeting the container from 30 M to 2 M. The system was able to accommodate both negative and positive angles of the spreader based on the reference point (Figure 4, 5, and 6).

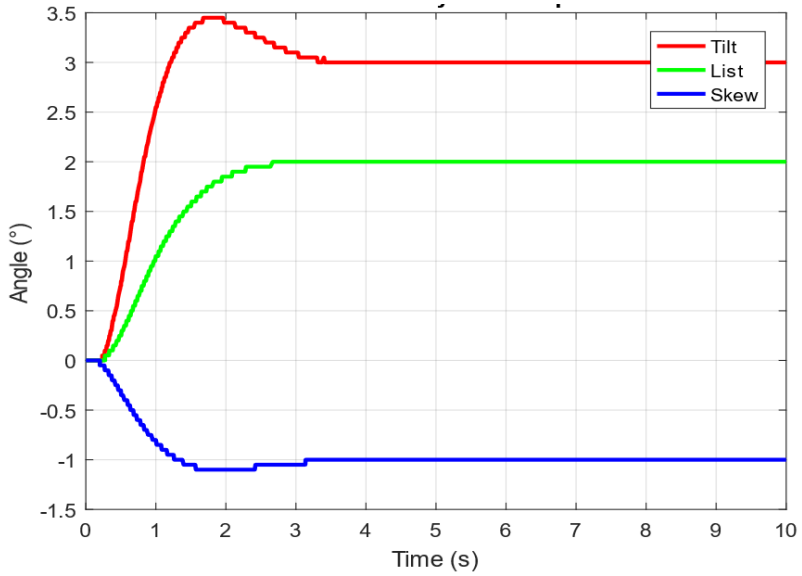

Figure 7. Spreader system output of sea-to-shore gantry crane full system response

From the height of 30 m, and at 7 m machine-vision was activated as cameras kept on monitoring the spreader position aligned with the targeted container corner casts. At 6.5 m a tilt, list and skew were detected and controllers initiated the correction and spreader angle was adjusted smoothly as shown in Figure 8. Alignment stabilized before reaching the container and hence final landing at 2 m.

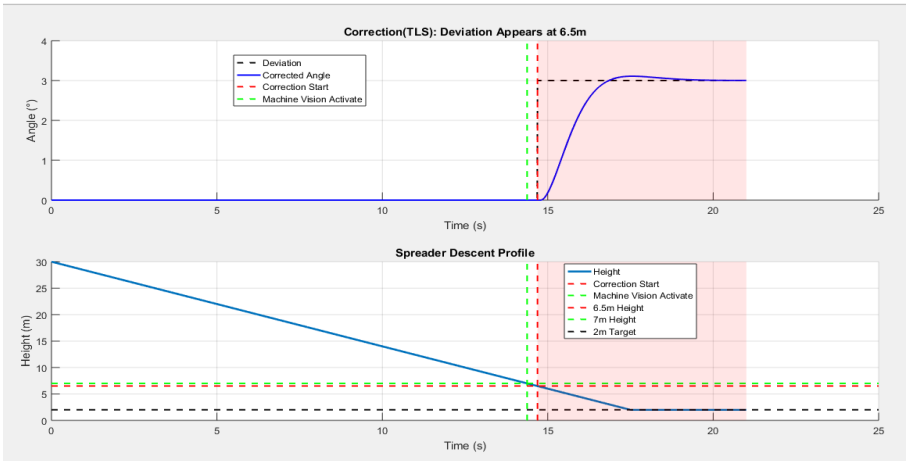

Figure 8. Spreader Correction for Tilt, List and Skew

Published, June 2026

Integrated results for tilt, list and skew

The Integrator System implemented as shown in Figure 3 corresponds with the results in Figure 9 in a specialized Simulink-based control subsystem, developed using a MATLAB Function Block. Its primary objective was to integrate and coordinate the dynamic behaviors of list, tilt, and skew three critical parameters that influence the stability and operational accuracy of ship-to-shore (STS) gantry cranes. This integration was essential to ensure synchronized and safe movement of the spreader of the crane during container handling operations.

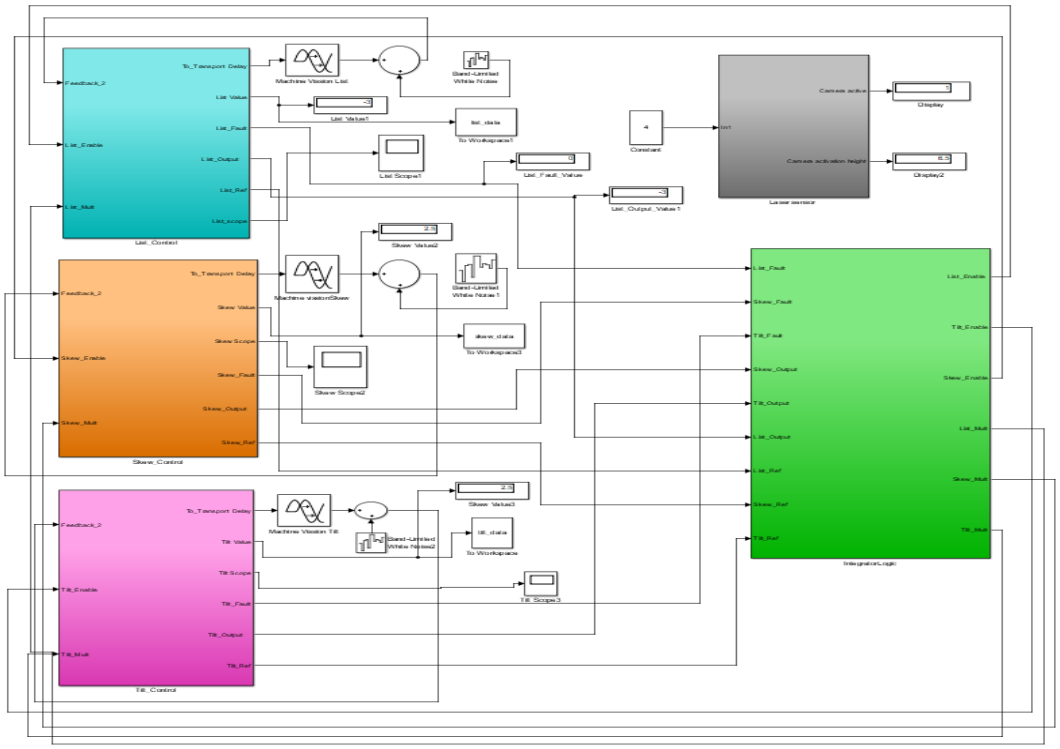

Figure 9. Combination of Tilt, List and Skew from an Integrator

The system was designed to act as an intelligent supervisory controller, particularly active when the deviations in tilt, list, or skew exceeded the acceptable operational threshold of ±3 degrees. In such cases, the Integrator temporarily overrode the standard PID controller output to regain control. This short-term override ensured that the spreader was realigned to a near-horizontal position where only minor angular adjustments were necessary, thereby improved interlock engagement efficiency and reducing mechanical stress on the system. Fast container coupling increased the number of moves leading to increase in productivity since operator used the standard speed of 45m per minute because of the spreader self-alignment to container corner casts. Fast loading and offloading of containers improved ship turn around reducing the number of vessels in the sea as waiters from 20 ships to 5 ships which was manageable meaning there was no need to expand the port in the near future.

Conclusion

In this paper, modified commands in controlling the spreader for correct placement on container saved time by limiting the sway angle and perfect introduction of tilt, list, and skew based on the reference angle picked by the cameras and machine vision interpretation. The only shortcoming identified was when the hydraulic level was low, the actuators (hydraulic cylinders) failed to make adjustments perfectly which was resolved by ensuring hydraulic level was at required limits. However, on safely spreader-container placement the system was more effective in fulfilling the objective of fast perfect spreader twist lock placement on container corner casts. By reducing the cycle per container,

Published, June 2026

it reduced the ship turn around hence increasing productivity. The number of vessels as waiters drastically reduced by 30%.

Acknowledgement

We express our sincere gratitude to the Kenya Ports Authority for invaluable support and collaboration throughout this study, all members of the Sea-to-Shore gantry cranes technical team and to all individuals whose contributions were instrumental in the successful completion of this study.

References

Ayper, B., & Pense, C. (2026). Container Stack Yard Optimization Using ALV Vehicles: The Case of TraPac LLC. *Journal of ETA Maritime Science*. https://doi.org/10.4274/jems.2025.27167.

Beller, S., & Yavuz, H. (2021). Crane automation and mechanical damping methods. *Alexandria Engineering Journal*, 60(3): 3275–3293 https://doi.org/10.1016/j.aej.2021.01.04

Cibicik, A., Myhre, T.A., & Egeland, O. (2018). Modeling and Control of a Bifilar Crane Payload. *2018 Annual American Control Conference (ACC)*, 1305–1312. https://doi.org/10.23919/ACC.2018.8431375

Galeani, S., Onori, S., Teel, A.R., & Zaccarian, L. (2008). A magnitude and rate saturation model and its use in the solution of a static anti-windup problem. *Systems & Control Letters*, 57(1): 1–9. https://doi.org/10.1016/j.sysconle.2007.06.011

Grypp, M.D., Marianno, C.M., Poston, J.W., & Hearn, G.C. (2014). Design of a spreader bar crane-mounted gamma-ray radiation detection system. *Nuclear Instruments and Methods in Physics Research Section A: Accelerators, Spectrometers, Detectors and Associated Equipment*, 743: 1–4. https://doi.org/10.1016/j.nima.2014.01.015

Jaafar, H.I., Mohamed, Z., Jamian, J.J., Abidin, A. F.Z., Kassim, A.M., & Ghani, Z.A. (2013). Dynamic Behaviour of a Nonlinear Gantry Crane System. *Procedia Technology*, 11: 419–425. https://doi.org/10.1016/j.protcy.2013.12.211

Kim, G.H., & Hong, K.S. (2019). Adaptive Sliding-Mode Control of an Offshore Container Crane With Unknown Disturbances. *IEEE/ASME Transactions on Mechatronics*, 24(6): 2850–2861. https://doi.org/10.1109/TMECH.2019.2946083

Li, Y., Li, S., Zhang, Q., Xiao, B., & Sun, Y. (2022). Application of Big Data Technology in Ship-to-Shore Quay Cranes at Smart Port. *Infrastructures*, 7(5): 73. https://doi.org/10.3390/infrastructures7050073

Masoud, Z.N., Nayfeh, A.H., & Mook, D.T. (2004). Cargo Pendulation Reduction of Ship-Mounted Cranes. *Nonlinear Dynamics*, 35(3): 299–311. https://doi.org/10.1023/b:nody.0000027917.37103.bc

Milazzo, M.F., Ancione, G., Brkic, V.S., & Vališ, D. (n.d.). *Investigation of crane operation safety by analysing main accident causes*.

Ngo, Q.H., & Hong, K.S. (2009). Skew control of a quay container crane. *Journal of Mechanical Science and Technology*, 23(12): 3332–3339. https://doi.org/10.1007/s12206-009-1020-1

Ngo, Q. H., Yu, Y., Kim, E.H., Jang, I.G., & Hong, K.-S. (n.d.). *Orientation control of a crane's spreader: Application on mobile harbor*.

Parra, L.A., & Tannuri, E.A. (2012). Definition and numerical simulation of an automated system for container crane positioning. *Control Systems*, 5.

Qian, Y.Z., Fang, Y.C., & Yang, T. (2018). An Energy-based Nonlinear Coupling Control for Offshore Ship-mounted Cranes. *International Journal of Automation and Computing*, 15(5): 570–581. https://doi.org/10.1007/s11633-018-1134-Y

Smid, G.E., Klaassens, J.B., Van Nauta Lemke, H. R., El Azzouzi, A., & Van Der Wekken, R. (2000). Automatic Skew Control on Container Transhipment Cranes. *IFAC Proceedings Volumes*, 33(26): 977–982. https://doi.org/10.1016/S1474-6670(17)39272-8